

NPY genes and AGC kinases define two key steps in auxin-mediated organogenesis in *Arabidopsis*

Youfa Cheng, Genji Qin, Xinhua Dai, and Yunde Zhao¹

Section of Cell and Developmental Biology, University of California at San Diego, 9500 Gilman Drive, La Jolla, CA 92093-0116

Edited by Winslow R. Briggs, Carnegie Institution of Washington, Stanford, CA, and approved November 18, 2008 (received for review September 30, 2008)

Auxin is an essential regulator of plant organogenesis. Most key genes in auxin biosynthesis, transport, and signaling belong to gene families, making it difficult to conduct genetic analysis of auxin action in plant development. Herein we report the functional analysis of several members of 2 gene families (NPY/ENP/MAB4 genes and AGC kinases) in auxin-mediated organogenesis and their relationships with the YUC family of flavin monooxygenases that are essential for auxin biosynthesis. We show that 5 NPY genes (NPY1 to NPY5) and 4 AGC kinases (PID, PID2, WAG1, and WAG2) have distinct, yet overlapping, expression patterns. Disruption of NPY1 does not cause obvious defects in organogenesis, but *np1 np3 np5* triple mutants failed to make flower primordia, a phenotype that is also observed when AGC kinase *PID* is compromised. Inactivation of *YUC1* and *YUC4* in *np1* background also phenocopies *np1 np3 np5* and *pid*. Simultaneous disruption of *PID* and its 3 closest homologs (*PID2*, *WAG1*, and *WAG2*) completely abolishes the formation of cotyledons, which phenocopies *np1 pid* double mutants and *yuc1 yuc4 pid* triple mutants. Our results demonstrate that NPY genes and AGC kinases define 2 key steps in a pathway that controls YUC-mediated organogenesis in *Arabidopsis*.

NPY1/ENP1/MAB4 | YUC | PINOID | embryogenesis | cotyledon

Formation of embryonic and postembryonic organs is an essential process for normal plant development and is regulated by intrinsic signals and environmental cues. Genetic analyses of *Arabidopsis* mutants with defects in organogenesis demonstrated that the plant hormone auxin plays a key role in determining the formation and patterning of lateral organs. Disruption of either auxin biosynthesis (1, 2) or polar auxin transport/auxin signaling (3–5) leads to defects in embryogenesis and in the formation of leaves and flowers. Auxin has been proposed as a morphogen that provides instructive signals for the formation of organs (6–9). The current model of organogenesis in *Arabidopsis* is that an auxin maximum (auxin peak) at the flanks of the apical meristem is necessary and sufficient to initiate the formation of lateral organs (9, 10). However, the exact mechanisms by which auxin regulates organogenesis are not fully resolved.

It is still not understood how auxin maxima are generated and maintained. Much of the work in this aspect in the past decade was centered on the active transport of auxin mediated by the PIN-FORMED (PIN) auxin efflux carriers and AUXIN1 (AUX1) influx carriers (4, 5, 10). Computer-assisted modeling on auxin dynamics and organogenesis based on PIN protein localization further improved our understanding of how auxin transport may contribute to the formation of auxin peaks (9, 11). However, recent progress in auxin biosynthesis reveals a more complicated picture. It appears that both local auxin production and polar auxin transport contribute to the creation and maintenance of auxin peaks. Mutations in the auxin efflux carrier *PIN1* disrupt the initiation of floral organs (5). Simultaneously inactivation of *YUCCA1* (*YUC1*) and *YUC4*, which encode homologous flavin-containing monooxygenases essential for de novo auxin biosynthesis (1, 12), also leads to defects in flower development (1). The *yuc1 yuc4 pin1* triple mutants fail to make

any true leaves (2), a phenotype not observed in either *pin1* or *yuc1 yuc4* alone, demonstrating that leaf initiation is controlled by both the auxin biosynthetic *YUC* genes and the auxin transport *PIN* genes. Furthermore, the auxin influx carrier mutant *aux1* itself does not show any defects in organogenesis in the aerial parts of *Arabidopsis*, but *aux1* fails to make flowers in the *yuc1 yuc2 yuc4 yuc6* quadruple-mutant background, indicating that the functions of AUX1 in organogenesis are masked by local auxin biosynthesis (2).

One of the difficulties in conducting genetic analysis of auxin pathways is that almost all of the key components in auxin biosynthesis, polar transport, and auxin signaling belong to gene families whose members have overlapping functions. For example, the 11 YUC flavin monooxygenases in *Arabidopsis* catalyze a rate-limiting step in auxin biosynthesis and disruption of a single *YUC* gene does not cause any obvious developmental defects, but some double- and triple-mutant combinations have severe defects in development (1, 12). For the PIN family of efflux carriers and the auxin response factor (ARF) family, inactivation of *PIN1* or MONOPTEROS (MP)/ARF5 alone is sufficient to cause dramatic developmental defects (5, 13, 14). However, it has been demonstrated that *PIN1* has overlapping functions with other *PIN* genes (4) and that *MP* has overlapping functions with *ARF7* and *ARF19* (15). Such genetic complexities in auxin pathways make it difficult to define the functions of an individual of a gene family and conduct epistasis analysis of the auxin mutants because inactivation of one gene does not lead to a complete null of the gene function because of the compensatory effects from the other homologous genes.

To further elucidate the molecular mechanisms by which auxin regulates plant organogenesis, we conducted a genetic screen for enhancers of *yuc1 yuc4* double mutants on the basis of the hypothesis that the *yuc1 yuc4* double mutants provide a sensitized background for identifying novel components that are involved in auxin-regulated organogenesis. Our previous studies have demonstrated that the *yuc* mutants synergistically interact with polar auxin transport mutants (2). We focused our attention to mutants that fail to make flowers, but still develop an inflorescence in the *yuc1 yuc4* background. Such naked inflorescences without flowers are called pin-like inflorescences. Formation of pin-like inflorescences has become a hallmark for malfunction of auxin pathways because known pin-like mutants such as *pin1* (5), *pinoid* (*pid*) (16, 17), and *mp* (14) all are involved in aspects of auxin biology.

We identified a *yuc1 yuc4* enhancer *naked pins in yuc mutants 1* (*np1*), which forms pin-like inflorescences in the *yuc1 yuc4* background, but not in wild-type background (18). Mutant *np1*

Author contributions: Y.C., G.Q., X.D., and Y.Z. designed research; Y.C., G.Q., X.D., and Y.Z. performed research; Y.C., G.Q., X.D., and Y.Z. analyzed data; and Y.C. and Y.Z. wrote the paper.

The authors declare no conflict of interest.

This article is a PNAS Direct Submission.

¹To whom correspondence should be addressed. E-mail: yzhao@biomail.ucsd.edu.

This article contains supporting information online at www.pnas.org/cgi/content/full/0809761106/DCSupplemental.

© 2008 by The National Academy of Sciences of the USA

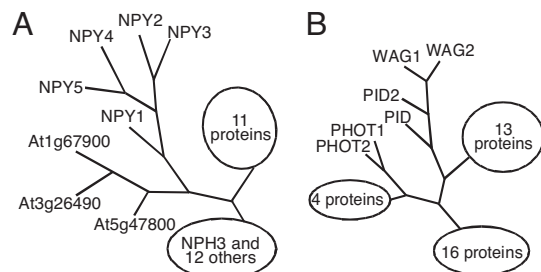


Fig. 1. Schematic trees of NPY proteins and AGC kinases. (A) A tree of NPY proteins that belong to a family with 32 members in *Arabidopsis*. The founding member of this superfamily is NPH3. For simplicity, the details of the NPH3 clade and the other large clade are not shown. (B) A tree of the AGC kinase family. More detailed phylogenetic trees of the 2 families have been published (18, 21, 24). The GenBank accession numbers for NPY genes are At4g31820 (NPY1), At2g14820 (NPY2), At5g67440 (NPY3), At2g23050 (NPY4), and At4g37590 (NPY5). The GenBank accession numbers for PID and its homologs are At2g34650 (PID), At2g26700 (PID2), At1g53700 (WAG1), and At3g14370 (WAG2).

is allelic to *enhancer of pinoid 1* (*enp1*) and *macchi-bou 4* (*mab4*) (19, 20), which failed to develop cotyledons in the *pid* background. *NPY1/ENP1/MAB4* encodes a plant-specific protein that contains a BTB (Bric-a-brac, Tramtrack, Broad-complex) domain at the N-terminal region and an NPH3 (NON-PHOTOTROPIC HYPOCOTYL 3) domain in the middle. NPY1 belongs to a large gene family with 32 members in the *Arabidopsis* genome (Fig. 1A). The founding member of this family, NPH3, mediates phototropic response downstream of the photoreceptor PHOT1 (21). Both PHOT1 and PID are Ser/Thr kinases that belong to the AGC kinase superfamily (Fig. 1B). The AGC kinases are the collective name for cAMP-dependent protein kinase A, cGMP-dependent protein kinase G, and phospholipids-dependent protein kinase C (22). The fact that NPY1 is homologous to NPH3 and PID is homologous to PHOT1 suggests that auxin-regulated organogenesis and phototropic responses are analogous. Furthermore, both processes require the involvement of an auxin response factor. Inactivation of NPH4/ARF7 leads to defects in phototropic response and disruption of MP/ARF5 leads to the formation of pin-like inflorescences (14, 23). Analysis of genetic interactions among *yuc1 yuc4*, *npyl*, and *pid* has put the genes in a genetic context in regulating *Arabidopsis* organogenesis (18).

The *npyl pid* double mutants and the *yuc1 yuc4 pid* triple mutants failed to make cotyledons, a phenotype that was not observed in *pid*, *npyl*, or *yuc1 yuc4* alone (18). The synergistic genetic interaction can be explained as the genes are involved in parallel pathways. Alternatively, it can also be interpreted that the YUCs, NPY1, and PID are in a linear pathway, providing that each gene has redundant partners in the *Arabidopsis* genome. To distinguish between the 2 possibilities, it is necessary to analyze whether other NPY1-like genes and PID-like genes also participate in auxin-regulated plant development. Herein we demonstrate that 2 closest NPY1 homologs in *Arabidopsis* also play an important role in the formation of flowers. Inactivation of one or more NPY1 homologs in *npyl* background leads to the formation of pin-like inflorescences, a phenotype observed in *pid* and *yuc1 yuc4 npyl* triple mutants (18). Furthermore, we show that inactivation of the 3 closest PID homologs in the *pid* background completely abolishes the formation of cotyledons, a phenotype that is also observed in *yuc1 yuc4 pid* triple mutants (18) and *npyl pid* double mutants (18, 19). Our analyses establish that members of YUC, NPY1, and PID families participate in a linear pathway in regulating auxin-mediated organogenesis in *Arabidopsis* and NPY genes and PID-like AGC kinases define 2 essential steps in the pathway. This study also provides a model

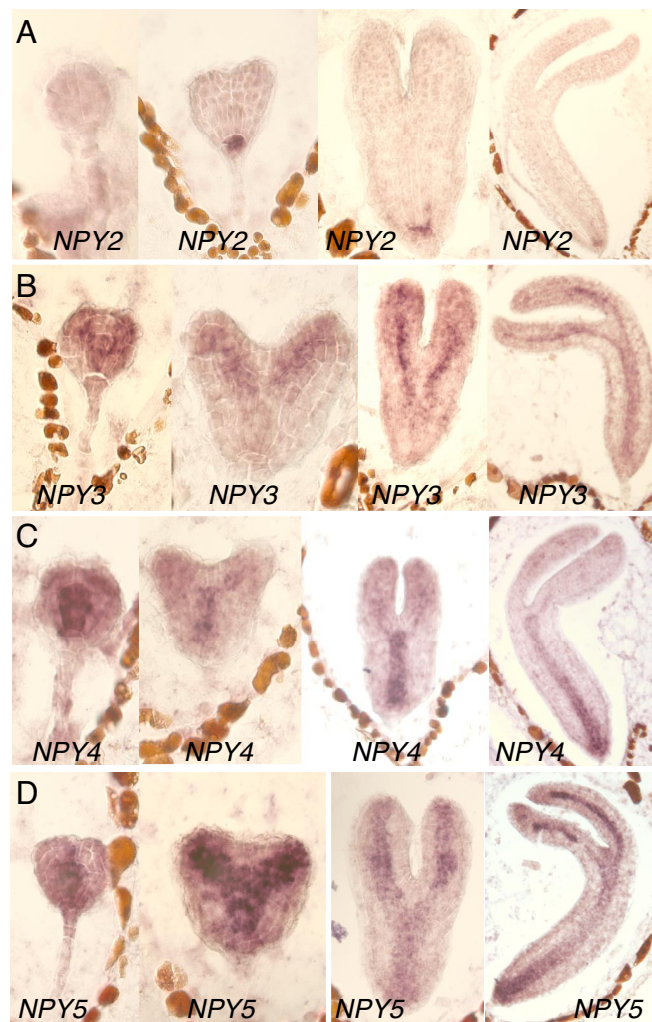


Fig. 2. The expression patterns of NPY genes during embryogenesis. (A) NPY2. (B) NPY3. (C) NPY4. (D) NPY5. The expression of the NPY genes were detected by using RNA in situ hybridization.

for conducting genetic analysis on a network of multiple gene families.

Results

NPY Genes Have Unique and Overlapping Expression Patterns. Mutations in NPY1 greatly enhanced the phenotypes of *yuc1 yuc4* double mutants (18) and *pid* mutants (18, 19), but *npyl* itself does not have dramatic developmental defects. It is likely that a subset of the NPY1 homologs has at least partially overlapping functions with NPY1. On the basis of sequence homology, the 32 members of the NPY1/NPH3 family in *Arabidopsis* can be divided into 4 subgroups: the NPH3/RPT2 group, the NPY group, and 2 other groups. In this article we focus our effort on the NPY group that includes 5 members named as NPY1 to NPY5 (Fig. 1A). Detailed phylogenetic analyses of the NPY1/NPH3 family and the AGC kinases have been described (18, 21, 24).

First, we analyzed the expression patterns of the 5 NPY genes by RNA in situ hybridization. It was evident that all 5 NPY genes were expressed during embryogenesis (Fig. 2) (18), but with distinct, yet overlapping, patterns. NPY1 was expressed mainly in the apical regions of embryos including cotyledon tips and the apical meristem (18). In contrast, NPY2 was specifically expressed in the hypophysis and the root meristems in the embryos (Fig. 2A). The expression of NPY3 was concentrated in provas-

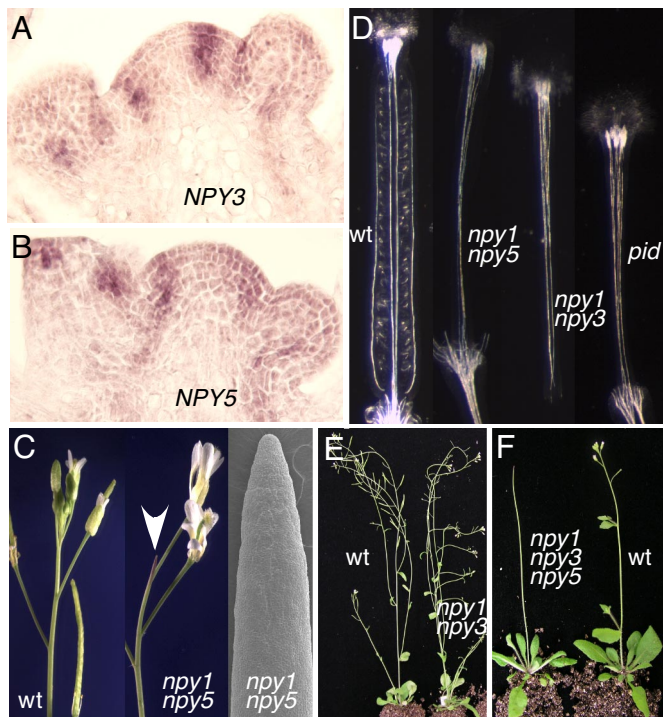


Fig. 3. The roles of *NPY* genes in *Arabidopsis* development. (A) Expression of *NPY3* in the inflorescence apex. (B) *NPY5* expression in the inflorescence apex. (C) Disruption of *NPY1* and *NPY5* led to the formation of pin-like inflorescences. A scanning electron microscope micrograph of *npy1 npy5* inflorescence is shown at right. The arrow points to a pin-like inflorescence. (D) *NPY* genes were required for proper gynoceium development. WT gynoceium had well connected and defined median and lateral vascular bundles. The ovules and valve tissues were also evident. However, *npy1 npy5*, or *npy1 npy3*, or *pid* all failed to make proper valves and developed abnormal vascular tissues in gynoceia. From left to right, WT, *npy1 npy5*, *npy1 npy3*, and *pid*. (E) The *npy1 npy3* double mutants were sterile. (F) The triple mutants of *npy1 npy3 npy5* formed strong pin-like inflorescences.

cular and vascular systems (Fig. 2B). Both *NPY4* and *NPY5* were also expressed in the cells that would differentiate into vascular bundles, but *NPY4* and *NPY5* appeared to have different tissue specificities (Fig. 2C and D). *NPY4* was expressed mainly in the hypocotyls (Fig. 2C), whereas *NPY5* was more concentrated in cotyledons (Fig. 2D). Overall, the expression of the 5 *NPY* genes marked the 2 meristems, provascular tissues, and the cotyledon tips during embryogenesis.

In the inflorescence apex, *NPY1* was expressed in the apical meristem and flower primordia (18). In apical meristem, the *NPY1* expression appeared to be restricted to the L1 layer (18). We did not detect any expression of *NPY2* in the inflorescence apex by RNA in situ hybridization (data not shown), which is consistent with the idea that *NPY2* may play a more specific role in root development. *NPY3* expression was not detected in the apical meristem; instead it marked the incipient sites of new floral primordia (Fig. 3A). *NPY3* mRNA was also detected in the early stages of flowers (Fig. 3A). *NPY4* was weakly expressed in the vascular tissues of inflorescences apex (data not shown). Among the 4 *NPY1* homologs, the expression pattern of *NPY5* was the most similar to that of *NPY1* (Fig. 3B) (18). *NPY5* mRNA was detected in the apical meristem and young flowers (Fig. 3B). However, *NPY5* showed a more pronounced expression in the incipient sites of flower primordia than *NPY1*. Overall, the expression patterns of *NPY5* overlapped greatly with those of *NPY1* and *NPY3* in the inflorescence apex.

Inactivation of *NPY* Genes Leads to the Formation of Pin-Like Inflorescences. We isolated T-DNA insertion mutants of *NPY1* and its 4 closest homologs (Fig. S1). None of the single mutants displayed any obvious defects in organogenesis except *npy1*, which had subtle defects in cotyledon development (18). The single *npy* mutants never developed pin-like inflorescences (data not shown). However, when *npy1* and *npy5* were combined, the resulting double mutants had pin-like inflorescences (Fig. 3C), a phenotype that was also observed in *pin1* (5), *pid*, *mp*, and *npy1 yuc1 yuc4* triple mutants. The *npy1 npy5* double mutants still made some flowers, but the flowers were abnormal (Fig. 3C). Like the flowers in *pid* and *pin1*, the *npy1 npy5* flowers often contained multiple petals (Fig. S2). The gynoceium of *npy1 npy5* often lacked valves and displayed vascular defects (Fig. 3D), which were also observed in *pid* and *pin1* mutants. The observed phenotypes of *npy1 npy5* correlated well with the fact that both *NPY1* and *NPY5* were expressed in the inflorescence meristem and that the expression patterns of the 2 genes overlapped (Fig. 3) (18).

The double mutants *npy1 npy3* also displayed defects in flower development (Fig. 3E). Inactivation of both *NPY1* and *NPY3* led to sterile plants (Fig. 3E). The flowers in *npy1 npy3* failed to develop proper valves and vascular tissues in gynoceium, phenotypes not observed in either *npy1* or *npy3* alone (Fig. 3D). The defects in gynoceium development in *npy1 npy3* double mutants were very similar to those observed in *npy1 npy5* and *pid* (Fig. 3D). The genetic enhancement of *npy1* by *npy3* indicated that *NPY1* and *NPY3* also had overlapping functions, which is consistent with the expression patterns of *NPY1* and *NPY3* (Fig. 3).

Interestingly, the double mutants of *npy3 npy5* did not display any obvious developmental defects, suggesting that *NPY1* plays a more prominent role. We generated all other possible double mutant combinations including *npy1 npy2* and *npy1 npy4*, but only *npy1 npy3* and *npy1 npy5* displayed obvious developmental defects. The triple mutants of *npy1 npy3 npy5* had stronger phenotypes than the double mutants *npy1 npy3* or *npy1 npy5* (Fig. 3F). The triple mutants made very few flowers and developed strong pin-like inflorescences (Fig. 3F). We further inactivated *NPY2* and *NPY4* in the *npy1 npy3 npy5* triple-mutant background; the resulting quintuple mutants were very similar to the *npy1 npy3 npy5* triple mutants.

Three *PID* Homologs Were Expressed During Embryogenesis. *PID* is expressed during *Arabidopsis* embryogenesis, and *PID* has been shown to play important roles in cotyledon development. Because both *npy1 pid* and *yuc1 yuc4 pid* failed to develop cotyledons while *pid* alone made cotyledons, we hypothesized that the *PID* homologs and *PID* may have overlapping functions in cotyledon development. In this article, we focus on the 3 closest *PID* homologs (*PID2*, *WAG1*, and *WAG2*) (Fig. 1B) and their roles in plant development. Both *WAG1* and *WAG2* were shown to play a role in root development and gravitropic response (25), whereas the role of *PID2* [previously called AGC1-10 or AGC3-4 (22, 24)] in plant development has not been analyzed.

We first used RNA in situ hybridization to investigate whether the *PID* homologs are expressed during embryogenesis. We detected the mRNAs of the 3 *PID* homologs during embryogenesis (Fig. 4). Both *WAG1* and *WAG2* were expressed throughout the embryogenesis; higher expression of *WAG1* and *WAG2* in the cotyledon primordia at heart stages was evident (Fig. 4). Compared with *WAG1* and *WAG2*, *PID2* had much higher expression (Fig. 4). The *PID2* mRNA was restricted mainly in provascular tissues (Fig. 4), a pattern that was very similar to those of *NPY3*, *NPY4*, and *NPY5* (Fig. 2).

***PID* and Its Homologs Are Essential for the Formation of Cotyledons.** We isolated T-DNA insertion mutants of *PID*, *PID2*, *WAG1*, and *WAG2* (Fig. S3). Inactivation of *PID* led to the formation of 3

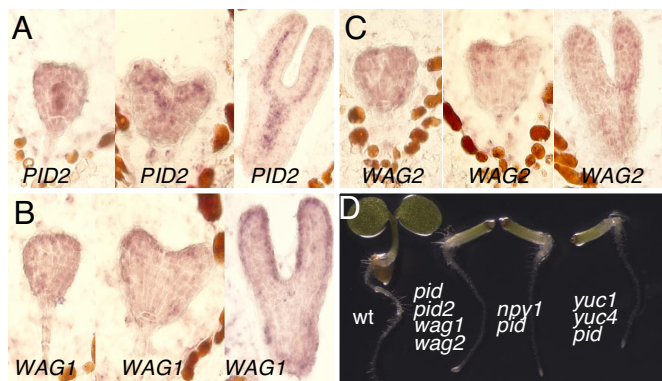


Fig. 4. The expression patterns of the 3 closest homologs of *PID* and their roles in embryogenesis. (A) *PID2* expression. (B) *WAG1* expression. (C) Expression pattern of *WAG2*; the expression patterns were revealed by in situ RNA hybridization. (D) Essential roles of *PID* and its homologs in cotyledon development. The quadruple mutants *pid pid2 wag1 wag2* failed to make cotyledons. The same phenotypes were also observed in *npy1 pid* and *yuc1 yuc4 pid*. From left to right, WT, *pid pid2 wag1 wag2* quadruple mutants, *npy1 pid* double mutants, and *yuc1 yuc4 pid* triple mutants.

cotyledons, but the phenotype was not fully penetrant. Single mutants of *pid2*, *wag1*, and *wag2* did not display any obvious defects in embryogenesis (data not shown). When we put *pid2* in *pid* background, the resulting double mutants behaved like *pid* during embryogenesis (Table 1). Most seedlings (72%) of the double mutants *pid wag1* had normal-looking cotyledons, but we observed some seedlings (24%) with only residual cotyledons or no cotyledon at all (1%) (Table 1) (Fig. S4). Like *pid wag1*, $\approx 5\%$ of *pid wag2* had residual cotyledons, 14% had no cotyledons, and 81% appeared normal. Other double mutants without *pid* such as *wag1 wag2* did not show obvious embryonic defects.

We also analyzed the triple-mutant combinations of *pid*, *pid2*, *wag1* and *wag2* (Table 1). Whereas *pid2 wag1 wag2* did not show any obvious defects, the other triple mutants displayed defects in cotyledon development. The majority of *pid pid2 wag1* and *pid pid2 wag2* had normal cotyledons (77% and 73%, respectively), and a small number of the triple mutants had cotyledon defects (Table 1). Unlike the other triple mutants, most of the *pid wag1 wag2* triple mutants (88%) failed to make any cotyledons and only 7% had residue cotyledons (Table 1). Less than 5% of *pid*

wag1 wag2 displayed normal cotyledons. We noticed that heterozygous *wag1* or *wag2* increased the frequency of cotyledon defects in *pid wag2* and *pid wag1*, respectively (Table 1). The no-cotyledon phenotype in *pid wag1 wag2* was identical to that of *npy1 pid* and *yuc1 yuc4 pid* (Fig. 4). The failure to make cotyledons in *pid wag1 wag2* took place during embryogenesis (Fig. S4).

We further analyzed the *pid pid2 wag1 wag2* quadruple mutants. Among the 59 seedlings of the quadruple mutants, 58 seedlings had no cotyledons, suggesting the phenotype was almost fully penetrant (Table 1). Our genetic analyses indicate that *PID* plays a more prominent role than the *PID* homologs during embryogenesis. Whereas the majority of *pid wag1 wag2* did not make cotyledons (88%), the frequency was greatly increased (98%) in *pid pid2 wag1 wag2*.

Discussion

Herein we present direct evidence that the *NPY* genes play an essential role in *Arabidopsis* organogenesis. Our genetic analysis of *NPY* genes and *PID* genes demonstrates that each gene family represents a key step in exerting the functions of auxin during *Arabidopsis* development.

***NPY* Genes Collectively Control Organogenesis in *Arabidopsis*.** *NPY1* belongs to a large gene family (Fig. 1A). Genetic screens for enhancers of *yuc1 yuc4* and *pid* led to the discovery of *NPY1* as a key component in auxin-regulated organogenesis. The *npy1 pid* double mutants failed to develop cotyledons and the *npy1 yuc1 yuc4* formed pin-like inflorescences (18), but *npy1* alone did not display obvious developmental defects. In addition to the interpretation that *NPY1* works in the same pathway as *PID* and *YUC* genes, the observed genetic enhancements among *yuc*, *pid*, and *npy1* can be accounted for if *NPY1* and *PID* function in parallel pathways. Inactivation of either *NPY3* or *NPY5* in the *npy1* background led to dramatic flower defects similar to those observed in *pid* (Fig. 3). Furthermore, the *npy1 npy3 npy5* display strong pin-like phenotypes (Fig. 3), which is identical to those of strong *pid* alleles, demonstrating that *NPY1* and *PID* are unlikely to function in 2 parallel pathways.

NPY1, *NPY3*, and *NPY5* displayed overlapping and distinct expression patterns (Figs. 2 and 3), suggesting that each gene may also have unique functions. It is difficult to dissect the unique functions of the genes in a family. It may require us to put individual mutants in a sensitized background. For example,

Table 1. Genetic analyses of mutant combinations of *pid*, *pid2*, *wag1*, and *wag2*

Parent genotype	Mutant genotype	Mutant genotype analysis			Mutant phenotype analysis		
		No. of seedlings (% of total seedlings genotyped)		Seedlings genotyped	No. of seedlings (% of total number of mutant seedlings)		
		Expected	Observed			With cotyledons	Residual cotyledons
<i>pid^{+/-} pid2</i>	<i>pid pid2</i>	36 (25)	33 (23)	144	33 (100)	0 (0)	0 (0)
<i>Pid^{+/-} wag1</i>	<i>pid wag1</i>	27 (25)	25 (23)	109	18 (72)	6 (24)	1 (4)
<i>pid^{+/-} wag2</i>	<i>pid wag2</i>	40 (25)	37 (23)	160	30 (81)	2 (5)	5 (14)
<i>pid^{+/-} pid2 wag1^{+/-}</i>	<i>pid pid2 wag1</i>	10 (6)	13 (8)	164	10 (77)	1 (8)	2 (15)
<i>pid^{+/-} pid2^{+/-} wag2</i>	<i>pid pid2 wag2</i>	>9(>6)*	26 (18)	145	19 (73)	3 (12)	4 (15)
<i>pid^{+/-} wag1^{+/-} wag2</i>	<i>pid wag1 wag2</i>	8 (6)	7 (6)	121	0 (0)	0 (0)	7 (100)
<i>pid^{+/-} wag1 wag2^{+/-}</i>	<i>pid wag1 wag2</i>	8 (6)	5 (4)	135	0 (0)	0 (0)	5 (100)
<i>pid^{+/-} wag1 wag2</i>	<i>pid wag1 wag2</i>	29 (25)	30 (26)	116	2 (7)	3 (10)	25 (83)
<i>pid^{+/-} wag1 wag2^{+/-}</i>	<i>pid wag1 wag2^{+/-}</i>	17 (13)	12 (9)	135	1(8)	4 (33)	7 (58)
<i>pid^{+/-} wag1^{+/-} wag2</i>	<i>pidwag1^{+/-} wag2</i>	15 (13)	18 (15)	121	2 (11)	3 (17)	13 (72)
<i>pid2 wag1 wag2</i>	<i>pid2 wag1 wag2</i>	24 (100)	24 (100)	24	24 (100)	0 (0)	0 (0)
<i>pid^{+/-} pid2 wag1 wag2</i>	<i>pid pid2 wag1wag2</i>	59 (25)	59 (25)	237	1 (2)	0 (0)	58 (98)

*Both *PID* and *PID2* are located on chromosome II and are linked.

YUC1 and *YUC4* have overlapping and unique expression patterns and the 2 genes certainly have overlapping functions (1). However, when combined with *pin1-5*, *yuc4 pin1-5* double mutants displayed a much stronger phenotype than *yuc1 pin1-5*, indicating that *YUC4* plays a more prominent role in inflorescence development than *YUC1* (2). It will be interesting to investigate whether other *NPY* genes can also enhance *yuc1 yuc4* and *pid*.

NPY2 and *NPY4* were expressed in *Arabidopsis* (Fig. 2), but so far we have not had direct evidence that the 2 genes are also involved in auxin-regulated plant development. It is striking that *NPY2* was specifically expressed only in the root meristem (Fig. 2A), indicating that *NPY2* may have a root-specific function. As discussed previously, *npyl pid* double mutants had severe defects in cotyledon development; however, *npyl npy2 npy3 npy4 npy5* quintuple mutants did not display obvious defects in embryogenesis, suggesting that additional *NPY* genes may also participate in embryogenesis. The obvious candidates would be the 3 genes that have the highest homology to the *NPY* clade (Fig. 1A). Furthermore, vascular development in cotyledons was disrupted when At5g10250, a distant homolog of *NPY1*, was mutated, suggesting that more *NPH3/NPY-like* genes may be involved in auxin-mediated plant development (26).

Control of Cotyledon Development by AGC Kinases. *PID* is known mainly for its role in the formation of flowers (16, 17). The fact that simultaneous inactivation of *PID* and its 3 closest homologs in *Arabidopsis* abolished the formation of cotyledons (Fig. 4D) demonstrates that the *PID* genes are also essential for cotyledon development. Remarkably, *pid pid2 wag1 wag2* is phenotypically indistinguishable from *npyl pid* and *yuc1 yuc4 pid* (Fig. 4D). Because *PID* is not a homolog of *NPY1* and *YUC* genes, the genetic enhancement of *pid* by *npyl* or *yuc1 yuc4* cannot be explained by gene redundancy. Therefore, we conclude *YUC* genes, *PID*, and *NPY* genes probably are key components in the same pathway involved in regulating organogenesis.

Interestingly, the *pid pid2 wag1 wag2* appear to be able to develop a primary root (Fig. 4D), whereas *yuc1 yuc4 yuc10 yuc11* failed to make a root meristem during embryogenesis. Therefore, it is likely that additional AGC kinases may be required for the root development (Fig. 1B). It will require us to make the right combinations of AGC kinases to observe defects in other processes.

A Pathway for Auxin-Regulated Organogenesis. Because *YUCs*, *NPYs*, and *PIDs* all belong to gene families, it is difficult to genetically determine whether they are in the same pathway. It is also difficult to conduct epistatic studies to determine the relative positions of the genes in a pathway. It is clear that members in each of the 3 families have overlapping functions. Plants with multiple *YUC* genes inactivated have much stronger phenotypes than the single mutants (1, 2). The same is true for the *PID* family and *NPY* family (Figs. 3 and 4). If the 3 families participate in the same pathway and are not involved in other pathways, we expect that removal of all *YUC* genes should lead to the same phenotypes as those caused by disruption of all *NPY* genes or *PID* genes. Although mutants without any *YUC* or *NPY* or *PID* activities are not available, our analysis on *yuc*, *pid*, and *npyl* mutant combinations and the genetic interactions among the 3 groups of mutants indicate that the 3 family genes are key components of a pathway that regulates auxin-mediated organogenesis. First, *pid* and *npyl npy5* displayed very similar defects in flower development: both formed pin-like inflorescences and abnormal flowers (Fig. 3). The defects in gynoecium of *npyl npy5* were also similar to those in *pid* and *yuc1 yuc4* quadruple mutants (1), demonstrating that mutations in each gene family lead to similar developmental defects. Second, the formation of cotyledons was completely disrupted by simultaneously inactivating

PID, *PID2*, *WAG1*, and *WAG2*. The same cotyledon defects can also be achieved by disrupting both *PID* and *NPY1* or inactivating *YUC1*, *YUC4*, and *PID* simultaneously. We propose that the 3 gene families participate in a linear pathway that regulates auxin-mediated organogenesis. *PID* and its 3 closest homologs are required for the formation of cotyledons. *PID* appears to be the most prominent member in the family because *pid* alone has flower defects and inactivating *pid2*, *wag1*, and *wag2* does not result in defects in flower development. *NPY1* and its homologs *NPY3* and *NPY5* are required for organogenesis (Fig. 3). Simultaneously inactivating *PID* and *NPY1* would effectively cut the output of the pathway to the level of multiple *pid* mutants. For example, if *PID* accounts for 70% of the output of the *PID* family and *NPY1* accounts for 70% of the output of the *NPY* family, the *npyl pid* double mutants will cut down the total output of the pathway to 9% if the 2 families work in the same pathway. The total output of the pathway in *pid* mutant background can also be further decreased if additional *PID* homologs are inactivated, which explains why *npyl pid* and *pid pid2 wag1 wag3* displayed identical cotyledon phenotypes. The same interpretation can also be applied to the synergistic genetic interactions between *yuc1 yuc4* and *pid*.

Our data support that *YUCs*, *PIDs*, and *NPYs* are components of a linear pathway that controls auxin-mediated organogenesis. However, the relative positions of the 3 gene families in the pathway have not been determined. Because *PID/NPY*-mediated organogenesis is analogous to *PHOT1/NPH3*-mediated phototropic responses where *PHOT1* is upstream of *NPH3*, we propose that *PID* is probably upstream of *NPY1*. Interestingly, *NPH3* physically interacts with the chromophore-binding portion of *PHOT1* to form a protein complex (21, 27). Unlike *PHOT1*, *PID* and its close homologs do not have the photoreceptor domain, suggesting that additional adaptor proteins may be involved in the *PID/NPY* pathway. Consistent with this hypothesis, preliminary studies indicate that *PID* and *NPY1* do not interact directly (19).

This work has put the complex genetic interactions among *YUCs*, *PIDs*, and *NPYs* into a simple pathway that provides a genetic basis for further understanding of how auxin regulates plant organogenesis. For example, it now becomes feasible to determine the relative positions of the components by gain-of-function studies in the various mutant backgrounds. Our genetic analysis on the gene families shown here also provides a model for analyzing complex genetic interactions among multiple gene families in other pathways.

Methods

Plant Materials. The T-DNA insertion mutants were obtained from the *Arabidopsis* Biological Resource Center or The Nottingham *Arabidopsis* Stock Center (NASC). The *npyl* mutant used in this study was the *npyl-2* T-DNA allele (SALK-108406), which has been described (18). The *npy2* mutant was the T-DNA line SALK-142094, which contained a T-DNA insertion in the first intron of the gene 75 bp after the ATG start codon. The *npy3* mutant referred to the T-DNA line SALK-119048. The T-DNA was inserted in the second exon of *NPY3*, 876 bp downstream of the ATG start codon. The *npy4* mutant was the SALK-046452 line, in which the T-DNA was inserted in the fourth exon, 1,628 bp downstream of the ATG start codon of *NPY4*. The *npy5* mutant was the T-DNA line N372878, a GABI-Kat line (GK-027H10) from NASC. The T-DNA was inserted in the fourth exon, 1,746 bp after the start codon of *NPY5*.

The T-DNA mutants were genotyped by using 3 primers according to the protocol described (28). For *npyl*, *npy2*, *npy3*, and *npy4*, the mutants were genotyped by using 2 gene-specific primers and 1 T-DNA-specific primer JMLB1. The T-DNA-specific primer for genotyping the T-DNA insertion site in *npy5* was PAC106-T-DNA (5'-ATATTGACCATCATACTCATTGC-3'). The gene-specific primers for genotyping *npyl* mutants are shown in Table S1.

The mutants for *pid* and its homologs all were T-DNA lines. The *pid* allele was the SALK-049736 line as reported (18). The *pid2* allele referred to the line SAIL-269-G07, in which a T-DNA fragment was inserted at 2,010 bp downstream of the ATG start codon of *PID2*. The *wag1* mutant referred to the SALK-002056. The T-DNA insertion was at 372 bp after the ATG start

codon of *WAG1*. The T-DNA allele of *wag2* was the line SALK-070240, which had a T-DNA insertion at 207 bp downstream of the ATG start codon of *WAG2*. The T-DNA-specific primer for genotyping *wag1* and *wag2* was the JMLB1, and the T-DNA-specific primer for *pid2* was SAIL-LB1 (5'-GCCTTTTC-AGAAATGGATAAATAGCCTTGCTTCC-3'). The gene specific primers for genotyping the PID homolog mutants are listed in Table S1.

Methods. We conducted the in situ RNA hybridization according to the methods described (29). The full-length cDNA of *NPY* and *PID* genes were used

as probes for the in situ hybridization. For in situ hybridization, at least 10 embryos with similar expression patterns were analyzed. Vascular visualization was performed by using protocols from ref. 1.

ACKNOWLEDGMENTS. We thank F. Pierri, S. Lee, A. Fang, Y. Liu, Y. Sun, M. Lewis, C. Won, and D. Ashak for DNA preparations and genotyping of various mutants and J. Du for helpful comments on the manuscript. This work was supported by National Institutes of Health Grant R01GM68631 (to Y.Z.).

1. Cheng Y, Dai X, Zhao Y (2006) Auxin biosynthesis by the YUCCA flavin monooxygenases controls the formation of floral organs and vascular tissues in *Arabidopsis*. *Genes Dev* 20:1790–1799.
2. Cheng Y, Dai X, Zhao Y (2007) Auxin synthesized by the YUCCA flavin monooxygenases is essential for embryogenesis and leaf formation in *Arabidopsis*. *Plant Cell* 19:2430–2439.
3. Dharmasiri N, et al. (2005) Plant development is regulated by a family of auxin receptor F box proteins. *Dev Cell* 9:109–119.
4. Friml J, et al. (2003) Efflux-dependent auxin gradients establish the apical-basal axis of *Arabidopsis*. *Nature* 426:147–153.
5. Galweiler L, et al. (1998) Regulation of polar auxin transport by AtPIN1 in *Arabidopsis* vascular tissue. *Science* 282:2226–2230.
6. Aida M, Tasaka M (2006) Genetic control of shoot organ boundaries. *Curr Opin Plant Biol* 9:72–77.
7. Heisler MG, Jonsson H. (2007) Modeling meristem development in plants. *Curr Opin Plant Biol* 10:92–97.
8. Nawy T, Lukowitz W, Bayer M. (2008) Talk global, act local—patterning the *Arabidopsis* embryo. *Curr Opin Plant Biol* 11:28–33.
9. Prusinkiewicz P, Rolland-Lagan AG (2006) Modeling plant morphogenesis. *Curr Opin Plant Biol* 9:83–88.
10. Reinhardt D, Mandel T, Kuhlemeier C (2000) Auxin regulates the initiation and radial position of plant lateral organs. *Plant Cell* 12:507–518.
11. Smith RS, et al. (2006) A plausible model of phyllotaxis. *Proc Natl Acad Sci USA* 103:1301–1306.
12. Zhao Y, et al. (2001) A role for flavin monooxygenase-like enzymes in auxin biosynthesis. *Science* 291:306–309.
13. Hamann T, Mayer U, Jurgens G (1999) The auxin-insensitive bodenlos mutation affects primary root formation and apical-basal patterning in the *Arabidopsis* embryo. *Development* 126:1387–1395.
14. Przemek GK, et al. (1996) Studies on the role of the *Arabidopsis* gene *MONOPTEROS* in vascular development and plant cell axialization. *Planta* 200:229–237.
15. Hardtke CS, et al. (2004) Overlapping and nonredundant functions of the *Arabidopsis* auxin response factors *MONOPTEROS* and *NONPHOTOTROPIC HYPOCOTYL 4*. *Development* 131:1089–1100.
16. Bennett SRM, Alvarez J, Bossinger G, Smyth DG (1995) Morphogenesis in pinoid mutants of *Arabidopsis thaliana*. *Plant J* 8:505–520.
17. Christensen SK, Dagenais N, Chory J, Weigel D. (2000) Regulation of auxin response by the protein kinase PINOID. *Cell* 100:469–478.
18. Cheng Y, Qin G, Dai X, Zhao Y (2007) NPY1, a BTB-NPH3-like protein, plays a critical role in auxin-regulated organogenesis in *Arabidopsis*. *Proc Natl Acad Sci USA* 104:18825–18829.
19. Furutani M, et al. (2007) The gene *MACCHI-BOU 4/ENHANCER OF PINOID* encodes a NPH3-like protein and reveals similarities between organogenesis and phototropism at the molecular level. *Development* 134:3849–3859.
20. Trembl BS, et al. (2005) The gene *ENHANCER OF PINOID* controls cotyledon development in the *Arabidopsis* embryo. *Development* 132:4063–4074.
21. Motchoulski A, Liscum E (1999) *Arabidopsis* NPH3: A NPH1 photoreceptor-interacting protein essential for phototropism. *Science* 286:961–964.
22. Bogre L, Okresz L, Henriques R, Anthony RG (2003) Growth signaling pathways in *Arabidopsis* and the AGC protein kinases. *Trends Plants Sci* 8:424–431.
23. Harper RM, et al. (2000) The NPH4 locus encodes the auxin response factor ARF7, a conditional regulator of differential growth in aerial *Arabidopsis* tissue. *Plant Cell* 12:757–770.
24. Galvan-Ampudia CS, Offringa R (2007) Plant evolution: AGC kinases tell the auxin tale. *Trends Plants Sci* 12:541–547.
25. Santner AA, Watson JC (2006) The *WAG1* and *WAG2* protein kinases negatively regulate root waving in *Arabidopsis*. *Plant J* 45:752–764.
26. Petricka JJ, Clay NK, Nelson TM (2008) Vein patterning screens and the defectively organized tributaries (dot) mutants in *Arabidopsis thaliana*. *Plant J* 56:251–263.
27. Pedmale UV, Liscum E (2007) Regulation of phototropic signaling in *Arabidopsis* via phosphorylation state changes in the phototropin 1-interacting protein NPH3. *J Biol Chem* 282:19992–20001.
28. Alonso JM, et al. (2003) Genomewide insertional mutagenesis of *Arabidopsis thaliana*. *Science* 301:653–657.
29. Dinneny JR, Weigel D, Yanofsky MF (2006) NUBBIN and JAGGED define stamen and carpel shape in *Arabidopsis*. *Development* 133:1645–1655.